

Ultrasonography of the pancreas.

4. Contrast-enhanced imaging

M. D'Onofrio,¹ G. Zamboni,¹ N. Faccioli,¹ P. Capelli,² R. Pozzi Mucelli¹

¹Department of Radiology, G.B. Rossi Hospital, University of Verona, Piazzale L.A. Scuro 10, 37134, Verona, Italy

²Department of Pathology, G.B. Rossi Hospital, University of Verona, Piazzale L.A. Scuro 10, 37134, Verona, Italy

Abstract

The introduction of contrast-enhanced ultrasonography (CEUS) has led to great developments in the diagnostic capabilities of ultrasound. Second generation contrast media, characterized by harmonic responses at low mechanical index of the ultrasound beam, have already proven usefulness in the study of the liver but other abdominal organs can take advantage from the dynamic study during continuous ultrasonographic scans. The dynamic observation of the enhancement allows the perfect evaluation of the abdominal organs perfusion. The perfusion of the pancreas is well correlated to the semeiology of the gland parenchymography at CEUS. The study of the pancreas is a new and promising application of CEUS. CEUS can be used to better identify pancreatic lesions respect to conventional Ultrasound (US) or to characterize pancreatic lesions already visible at US. Moreover the staging of some pancreatic lesions can be improved by the use of contrast media. This article will review the clinical application of CEUS in the different pancreatic pathologies.

Key words: Contrast-enhanced ultrasound—Mass-forming pancreatitis—Pancreatic tumors—Pancreatic pseudocyst—Pancreatic metastases

The introduction of contrast-enhanced ultrasonography (CEUS) has led to great developments in the diagnostic capabilities of ultrasound (US). Second-generation contrast media, characterized by harmonic responses at low acoustic pressures (low mechanical index) of the US beam, have already proven to be useful in the study of the liver, but examination of other abdominal organs can also benefit from the dynamic study during continuous ultrasonographic scans [1–3].

Study of the pancreas is a new and promising application of CEUS. CEUS can be used to better identify pancreatic lesions with respect to conventional US or to characterize pancreatic lesions already visible at US [4]. Moreover, the staging of some pancreatic lesions can be improved by the use of contrast media.

Technical background

Harmonic microbubble (MB)-specific imaging with a low acoustic US pressure is required for a dynamic CEUS examination using a second-generation contrast medium. While the background tissue signals are filtered by a specific algorithm of US image reconstruction, vascular enhancement signals in the regions of interest are related to the presence and the harmonic responses of the MBs. The enhancement at low-mechanical index harmonic imaging is immediately visible using second-generation US contrast media. Dynamic observation of the contrast-enhanced phases (early arterial, arterial, pancreatic, portal/venous, and late/sinusoidal phases) begins immediately after the injection of a second-generation contrast medium. Real-time evaluation of the enhancement is possible maintaining the same scanning frame rate as in the previous conventional B-mode examination [4]. Moreover, CEUS is the only imaging method that allows monitoring of the enhancement during the dynamic phases.

A number of technologies have been introduced for enhanced US imaging. Cadence coherent contrast imaging (Siemens-Acuson, Mountain View, CA, USA) is a filtered harmonic imaging technology based on inversion of the phase of alternate pulses. Summing up the resulting echoes, linear signals are canceled in favor of leaving nonlinear ones. Cadence contrast pulse sequencing (CPS; Siemens-Acuson) is a new and promising technology among recent technical developments in US detection of MB contrast agents. This technology takes advantage of the nonlinear fundamental imaging of

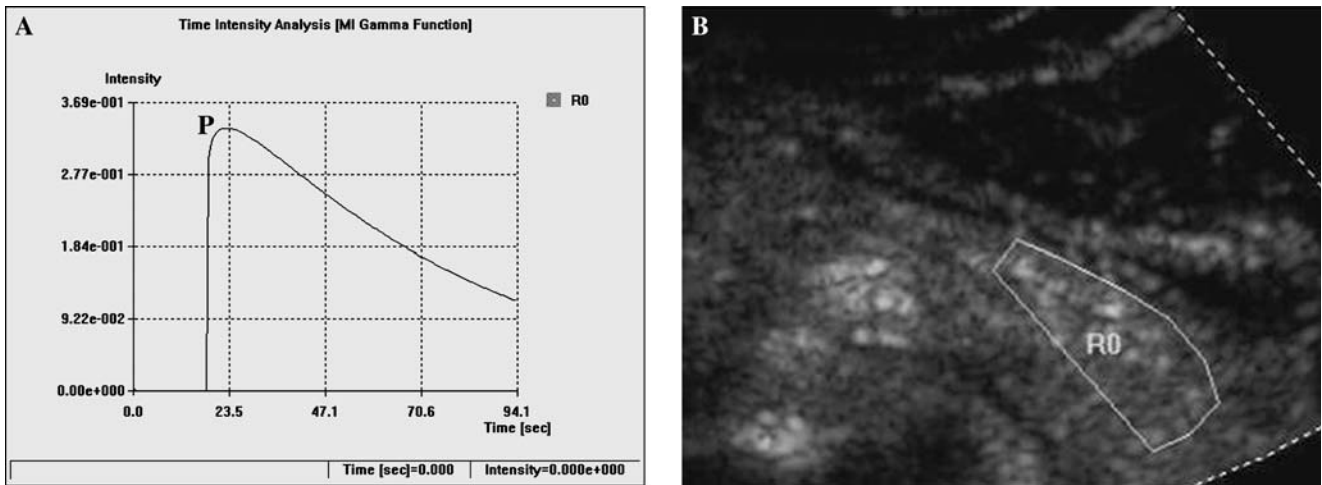


Fig. 1. Pancreatic perfusion. **A, B** CEUS: time–intensity curve of the pancreas obtained with a region of interest (R0 in B) placed at the pancreatic tail. The peak of enhancement (P) is reached about 20 s after contrast medium injection, after which a progressive washout is visible in the graphic.

MB resulting from precise changes in the amplitude and phase of transmitted pulses [5].

Sulfur hexafluoride MBs (SonoVue; Bracco, Milan, Italy) are a second-generation contrast medium with harmonic responses at low acoustic US pressures (mechanical index, <0.2). MBs are a blood pool contrast agent allowing pure arterial and venous vascular enhancement. In particular, MBs of sulfur hexafluoride (SonoVue) have a mean diameter of $2.5\ \mu\text{m}$, thus allowing them to reach the microcirculation [6]. Therefore the visualization of microvascular enhancement depends on the US spatial resolution. State-of-the-art US scanners have an optimal spatial resolution, thus allowing study of the microvasculature.

Examination protocols

The dynamic observation of enhancement allows perfect evaluation of abdominal organ perfusion. The perfusion of the pancreas is well correlated with the semiology of the gland parenchymography at CEUS. The differences in semiology between pancreatic CEUS study and the well-established liver CEUS study are substantial. In particular, considering that the blood supply of the pancreas is entirely arterial, the enhancement of the gland begins almost together with the aortic enhancement. At CEUS the enhancement reaches its peak between 15 and 20 s after contrast medium injection (Fig. 1). Pancreatic parenchymography is therefore earlier and shorter than that of the liver due to the absence of a venous blood supply like the portal one for the liver. CEUS of the pancreas shows a marked parenchymal enhancement in the early contrast-enhanced phases [7, 8]; afterward there is a progressive washout of contrast medium with loss of

gland echogenicity (Fig. 1). These considerations, while important for the interpretation of the enhancement patterns of pancreatic lesions, on the other hand, allow us to foresee difficulties in diagnostic imaging to obtain a correct lesion characterization: in fact there is often an unfavorable ratio between brevity of enhancement (“wash-in”) and contrast release (“wash-out”) of some pancreatic lesions compared to the quick parenchymography of the gland. The most important, unique feature of CEUS examination is its being continuous: it allows a continuous, dynamic observation of the contrast-enhanced phases, which facilitates identification of the fast-flow tumoral circulation [7].

The technique of contrast-enhanced ultrasonography of the pancreas should vary according to the clinical indications. To detect or study a small pancreatic lesion, to cover all the glandular sectors in the earliest contrastographic phases, two boli, each of 2.4 mL of contrast medium, and the “enhancement cancellation” technique by means of high-acoustic pressure flash can be employed [9, 10]. This technique, during the dynamic observation of the earliest contrastographic phases, almost completely eliminates saturation of the area immediately adjacent to the glandular parenchyma already studied, thus obtaining, again, a pure arterial phase. The relationship between the lesion and the main pancreatic duct has to be assessed.

To study and stage a large pancreatic lesion, after dynamic observation of the lesion during the arterial, pancreatic, and venous enhanced phases, judging its relation with the peripancreatic venous and arterial vessels, a complete evaluation of the liver during the late “sinusoidal” phase [4, 11, 12] must be performed to exclude the presence of liver metastases.

Clinical applications

Solid pancreatic lesions

Pancreatitis

Acute focal pancreatitis, even when supported by clinical data, can cause problems of differential diagnosis versus heteroplasic lesions [9, 10]. At US acute focal pancreatitis appears as a homogeneously hypoechoic segmental increase in volume of the pancreas [9, 10]. The inflamed pancreatic segment shows increased contrast enhancement at CEUS [10]. Therefore the presence of an increased parenchymography in the pancreatic lesion, resulting in an increase in echogenicity in the dynamic phases, may be a useful feature for differential diagnosis.

In severe acute pancreatitis CEUS may improve the identification and delimitation of areas of parenchymal necrosis, which appear as nonvascular areas [10].

Mass-forming chronic pancreatitis usually occurs in patients with a history of chronic pancreatitis [13]. Differential diagnosis with a neoplastic disease may be difficult not only because of the very similar ultrasonographic features [14], but also because mass-forming pancreatitis and pancreatic adenocarcinoma may present the same symptoms and signs [15]. The main characteristic feature at pathology is a progressive interstitial fibrosis with chronic inflammatory infiltrate [13]. US features of mass-forming pancreatitis are very similar to those of ductal adenocarcinoma [13, 14], presenting in most cases as a hypoechoic mass with enlargement of a limited sector of the gland, usually at the head (Fig. 2A). The presence of small calcifications in the lesion may suggest its inflammatory nature [16] but has a poor specificity. Contrast-enhanced examinations and biopsy are therefore mandatory for diagnosis. CEUS can improve US differential diagnosis between mass-forming pancreatitis and pancreatic adenocarcinoma. In particular, while ductal adenocarcinoma remains hypoechoic in all contrast-enhanced phases, as a consequence of its intense desmoplastic reaction with low mean vascular density, the inflammatory mass shows a “parenchymographic” enhancement in the early contrast-enhanced phase [10]. At CEUS, mass-forming pancreatitis shows “parenchymographic” enhancement (Fig. 2B) with lesional echogenicity similar to that of the surrounding parenchyma in the early phases; in the late phases enhancement decreases, with a washout rate similar to that of the pancreatic gland. The presence of a “parenchymography” somewhat similar to that of the adjacent pancreas during the dynamic study is therefore a CEUS finding consistent with an inflammatory origin. The intensity of this “parenchymographic” enhancement is related to the length of the underlying inflammatory process [10]. It has been observed that the more chronic and long-standing the inflammatory process is, the less intense is the intralesional “parenchymography,” prob-

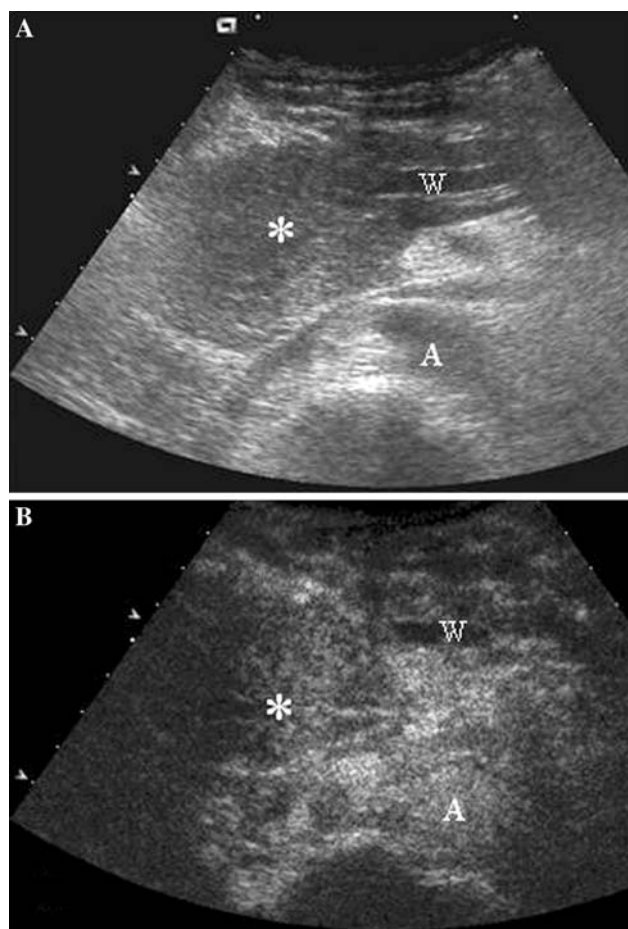


Fig. 2. Mass-forming chronic pancreatitis. **A** US: hypoechoic pancreatic head mass (*asterisk*) with upstream dilation of the main pancreatic duct (W). **B** CEUS: a “parenchymographic” enhancement of the lesion (*asterisk*), remaining isoechoic during all the dynamic phases, with enhancement somewhat similar to that of the adjacent pancreatic parenchyma. W, duct of Wirsung; A, aorta.

ably in relation to the entity of the associated fibrosis. On the contrary, in recent-onset mass-forming pancreatitis the enhancement is usually more intense and prolonged.

Autoimmune chronic pancreatitis is a particular type of chronic pancreatitis, with a very recent pathological definition: it is characterized by periductal flogosis, mainly sustained by lymphocytic infiltration, with evolution to fibrosis [17]. In comparison to other forms of chronic pancreatitis, the pancreas is increased in volume, usually in a diffuse way with the typical “sausage” look, and the main pancreatic duct is string-like, compressed by glandular parenchyma [17]. US features are very similar to those of focal pancreatitis, even though autoimmune pancreatitis may more frequently affect the entire gland or may present a larger extension and ubiquitous localization. US findings are characteristic in the diffuse form when the entire gland is involved (Fig. 3). Echogenicity is markedly reduced, gland volume

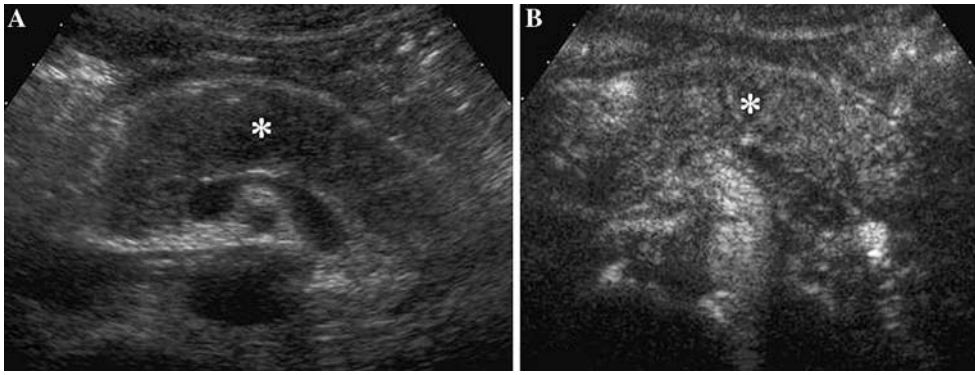


Fig. 3. Autoimmune chronic pancreatitis. **A** US: the pancreatic gland is diffusely hypoechoic (*asterisk*) and increased in volume. **B** CEUS: diffuse moderate inhomogeneous enhancement of the pancreatic gland (*asterisk*).

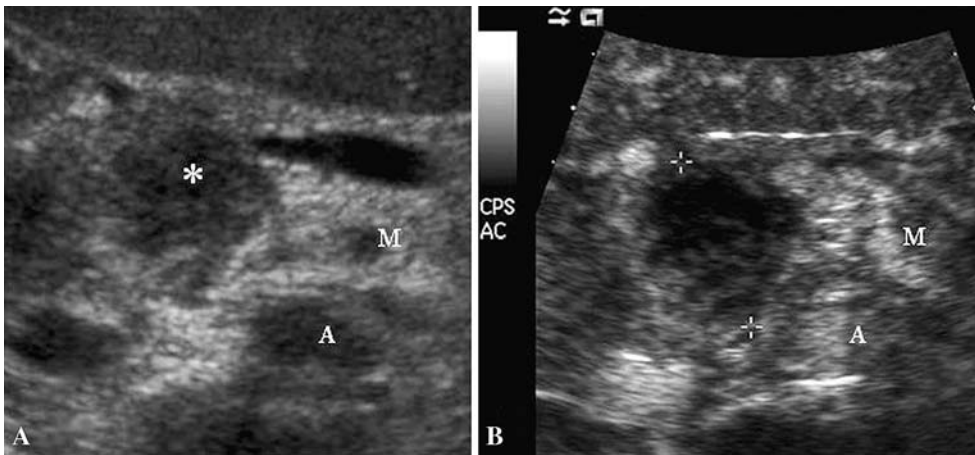


Fig. 4. Ductal adenocarcinoma. **A** US: hypoechoic pancreatic head mass (*asterisk*) with irregular margins infiltrating the splenomesenteric venous confluence. **B** CEUS: low enhancement of the mass (caliper), remaining hypoechoic in all the dynamic contrast-enhanced phases. M, superior mesenteric artery; A, aorta.

is increased, and the main pancreatic duct is compressed by glandular parenchyma (Fig. 3). Focal autoimmune pancreatitis at the pancreatic head is often characterized by the dilation only of the common bile duct [18]. The vascularization of autoimmune pancreatitis can be well demonstrated at CEUS (Fig. 3). CEUS of autoimmune pancreatitis shows a fair, moderate to marked [18], enhancement in the early contrast-enhanced phase (Fig. 3), though inhomogeneous for the thinning of the glandular vessels due to thick lymphocytic infiltration and fibrosis. Contrast medium washout is usually slow but progressive. CEUS findings may be especially useful in the study of focal forms of autoimmune chronic pancreatitis, in which differential diagnosis with ductal adenocarcinoma is a priority [19].

Neoplasms

Pancreatic tumors are classified according to their histological type and grade in the WHO classification [20]. *Ductal adenocarcinoma* comprises between 80% and 90% of all tumors of the exocrine pancreas. Ductal adenocarcinoma usually presents as a solid mass with infiltrative growth margins. US typically shows a hypoechoic lesion (Fig. 4) with ill-defined margins, confused with the adjacent parenchyma, often altering the gland contour or sometimes, when small, completely

included in the gland parenchyma. Ductal adenocarcinoma shows poor enhancement [18, 21, 22] in all CEUS phases (Fig. 4). At pathology the tumor is characterized by the presence of marked desmoplasia [20], which justifies its hard consistency (Fig. 5). Mean vascular density is low and often inferior to that of the normal pancreatic parenchyma [10, 23]. The marked desmoplasia (Fig. 5) and the low mean vascular density of the lesion, together with the possible presence of necrosis and mucin, justify its semiologic features [21]. At CEUS ductal adenocarcinoma presents as a hypoechoic mass (Fig. 4) compared to the adjacent normally enhancing pancreatic parenchyma; the margins and size of the lesion are better visible (Fig. 6), and also its relationship with peripancreatic arterial and venous vessels for local staging (Fig. 6).

The degree of differentiation of the adenocarcinoma influences its microvascular density (MVD) [24]. Poorly differentiated carcinoma has fair microvascular density and high malignancy, with regional and distant diffusion occurring earlier than with ductal adenocarcinoma. Pathology findings are represented by a large soft mass, with central necrotic areas. US features of poorly differentiated carcinoma are not univocal. It presents as a fair-sized hypoechoic lesion with central necrotic areas due to the rapid growth not supported by a sufficient, although marked, neoangiogenesis. Minute calcifications

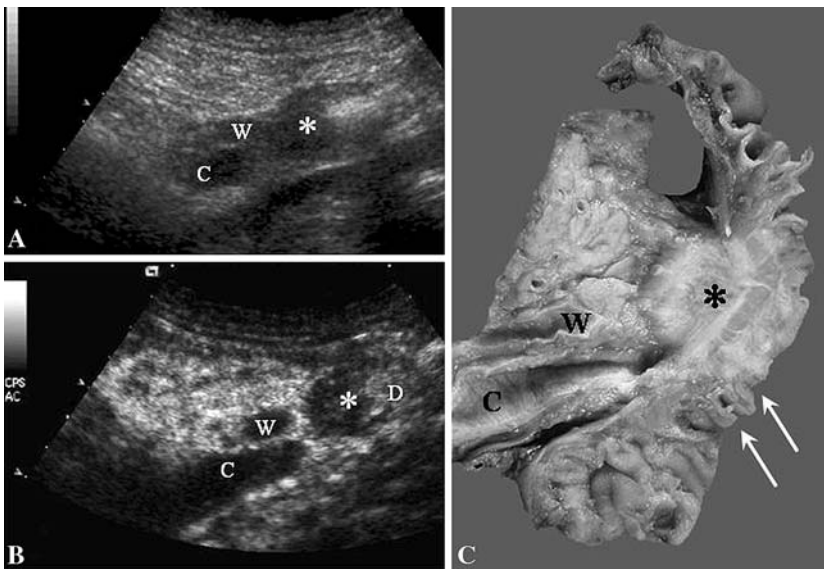


Fig. 5. Ductal adenocarcinoma. **A** US: longitudinal scan shows a dilated pancreatic duct (W) and a dilated common bile duct (C) (double duct sign). The two ducts end in a thick duodenal parietal wall (*asterisk*). **B** CEUS: the dynamic study shows that the Wirsung duct (W) and the common bile duct (C) are stopped in a small hypovascular mass (*asterisk*) infiltrating the duodenum (D). **C** Specimen: the main pancreatic duct (W) and the choleducus (C) are stopped in a small pancreatic ductal adenocarcinoma (*asterisk*) infiltrating the duodenal wall (*arrows*), with a perfect correlation with CEUS examination. The tumor is characterized by a high desmoplasia.

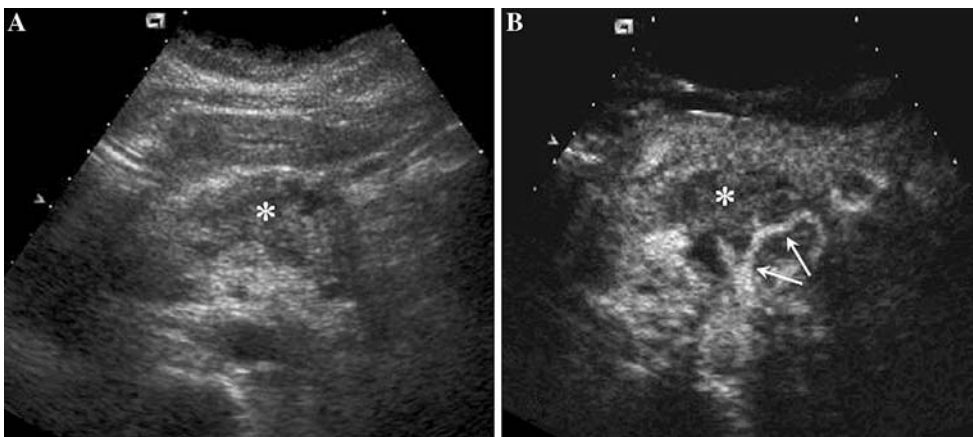


Fig. 6. Ductal adenocarcinoma. **A** US: axial scan showing an enlarged and extremely inhomogeneous pancreatic body (*asterisk*). **B** CEUS: the dynamic study revealed the presence of a hypovascular mass (*asterisk*) with encasement of the celiac and the splenic artery (*arrows*).

may be present in the intralesional necrotic areas. The tumor grows in all directions, usually in a concentric way. Vascular infiltration and regional and hepatic diffusion occur early. Color-Doppler and power-Doppler studies are not as accurate in the identification of tumoral vascularization. CEUS demonstrates the vascularization of the neoplastic tissue with enhancement already in the earliest phases of the dynamic study. Sometimes the enhancement of the viable tumor reveals a layer of solid tissue lining the intratumoral necrotic area, which appears nonvascular during the dynamic study. In the venous and late contrast-enhanced phases, after contrast medium washout, the viable portion of the tumor appears hypoechoic.

Endocrine tumors may induce specific clinical effects related to the tumoral released hormones (functioning endocrine tumors) or aspecific symptoms due to the expansive growth and tumor size (nonfunctioning endocrine tumors; NFETs). Endocrine tumors appear hypervascular at imaging [25]. Imaging differential

diagnosis between NFETs and ductal adenocarcinoma is fundamental for therapeutic strategy and prognosis [25]. At color- and power-Doppler ultrasonography a “spot pattern” can be demonstrated inside endocrine tumors [4]. However, Doppler “silence” can be present in hypervascular endocrine tumors because of the small size of the lesion or of the tumoral vascular network [4]. At CEUS different enhancement patterns can be observed in relation to the dimension of the tumor and tumoral vessels. Endocrine tumors show a rapid intense enhancement in the early contrast-enhanced phases (Fig. 7), with exclusion of the necrotic intralesional areas (Fig. 7), and MB entrapment in the late phase [4]. In moderate-size neuroendocrine pancreatic tumors a capillary blush enhancement can be present in the early contrast-enhanced phase, mirroring the most characteristic angiographic feature of this tumor [26], which becomes hypoechoic in the late contrast-enhanced phase [4]. Considering that the characterization of NFETs is mainly linked to their frequent hypervascularization

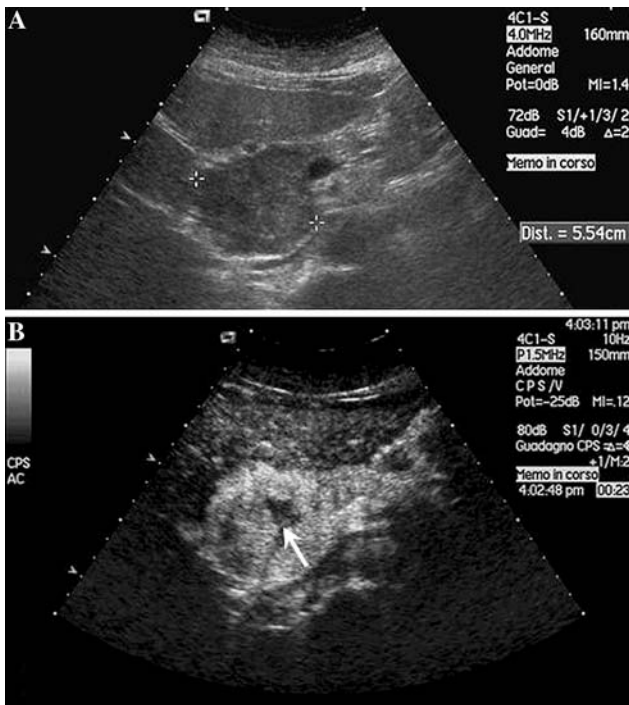


Fig. 7. Nonfunctioning endocrine tumor. **A** US: hypoechoic solid mass at the pancreatic head (caliper). **B** CEUS: rapid and intense enhancement of the lesion in the early contrast-enhanced phase, with small hypoechoic intratumoral necrotic areas (arrow).

[25], a high imaging modality sensitivity in detection of the macrocirculation and microcirculation of the lesion is required. Last but not least, NFETs can be hypovascularized [4]. This is directly related to the amount of stroma inside the lesion which is dense and hyalinized. However, in some pancreatic neuroendocrine tumors hypodense at spiral CT, a clear enhancement is visible at CEUS [4]. The high capability of CEUS to demonstrate pancreatic tumor vascularization [27] is a result of the high resolution power of state-of-the-art US imaging, combined with the size and distribution (blood pool) of the MBs. CEUS examination may improve the identification (Fig. 8) and characterization of endocrine tumors [4, 7]. CEUS examination, moreover, improves locoregional and hepatic staging of endocrine tumors [4].

Pancreatic metastases are rare; the most common are from renal cell carcinoma. CEUS may demonstrate enhancement of pancreatic metastases from renal carcinoma, as they are hypervascular (Fig. 9), allowing characterization and differential diagnosis versus pancreatic ductal adenocarcinoma [28, 29]. However, the CEUS features of pancreatic metastases from renal cell carcinoma can not be differentiated from those of endocrine tumors. The differential diagnosis is therefore based on the clinical history and symptomatology.

Cystic pancreatic lesions

Pseudocysts

Pseudocysts are the most common cystic lesions of the pancreas [30]. The lesion has a fibrous wall without an epithelial lining [30]. At imaging pseudocysts are more difficult to differentiate from cystic tumors of the pancreas, especially mucinous cystadenoma, whenever inclusions are present [30]. CEUS improves the ultrasonographic diagnosis of pseudocyst: differential diagnosis between pseudocysts and cystic tumors of the pancreas is more reliable thanks to the evaluation of intralesional inclusion vascularization. Pseudocysts are nonvascular and, therefore, do not show signal at CEUS (Fig. 10), becoming completely and homogeneously anechoic in the dynamic phase, even when showing a corpuscular and inhomogeneous content at basal US; the diagnosis of pseudocyst with intralesional debris is therefore possible (Fig. 10).

Neoplasms

Serous cystadenoma (SCA) usually has a benign nature [31]. The typical variety is microcystic, characterized macroscopically by multiple small cysts (<2 cm) separated by thin septa [30, 32, 33]. The margins are well defined and a central scar may be present [32]. CEUS improves the US characterization of SCA (Fig. 11), showing the enhancement of intralesional septa, with better identification of the microcystic features of the lesion [10]. The less common oligocystic and macrocystic types of serous cystadenoma present features undistinguishable from those of the other macrocystic tumors of the pancreas [34, 35].

Mucin-producing tumors of the pancreas may originate either from the peripheral ducts (mucinous cystic tumors) or from the main pancreatic duct and its collateral branches (intraductal papillary mucinous tumors; IPMTs) [36]. Mucinous cystadenoma (MCA), the most common cystic pancreatic tumor [37], is a rare primitive pancreatic tumor. MCA is considered a premalignant lesion [32, 38, 39], therefore a radiological characterization of MCA from other cystic pancreatic lesions is important for a correct therapeutic approach. MCA presents as a cystic round mass, multilocular or, less often, unilocular, of variable size (range: 2–36 cm) [40, 41]. The multilocular kind is typical, though not pathognomonic [42]. The unilocular type is less common and less specific and causes problems of differential diagnosis versus other cystic lesions of the pancreas [43], especially pseudocysts [32, 36, 39–42, 44–47] and the oligocystic variety of SCA [39]. MCA may present calcifications on the wall or the septa [48], parietal nodules, and papillary vegetations [41]. The cystic content of the lesion may be inhomogeneous [49] for the presence of mucin or intralesional hemorrhage. At US, MCA presents as a lesion

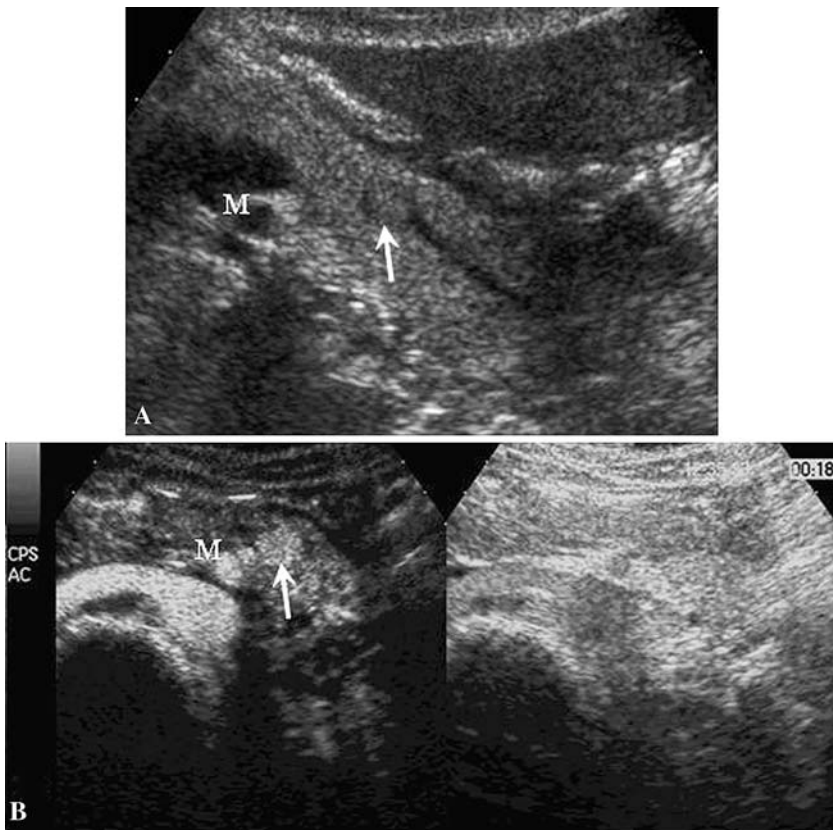


Fig. 8. Insulinoma. **A** US: oblique scan showing a small isoechoic nodule (*arrow*) inside the pancreatic body causing a slight dilatation of the main pancreatic duct. **B** CEUS: the dynamic study, performed with the “split-screen” software to correctly study the lesion, clearly demonstrated the rapid hypervascularization of the nodule, hyperechoic (*arrows*) to the adjacent pancreatic parenchyma. M, superior mesenteric artery.

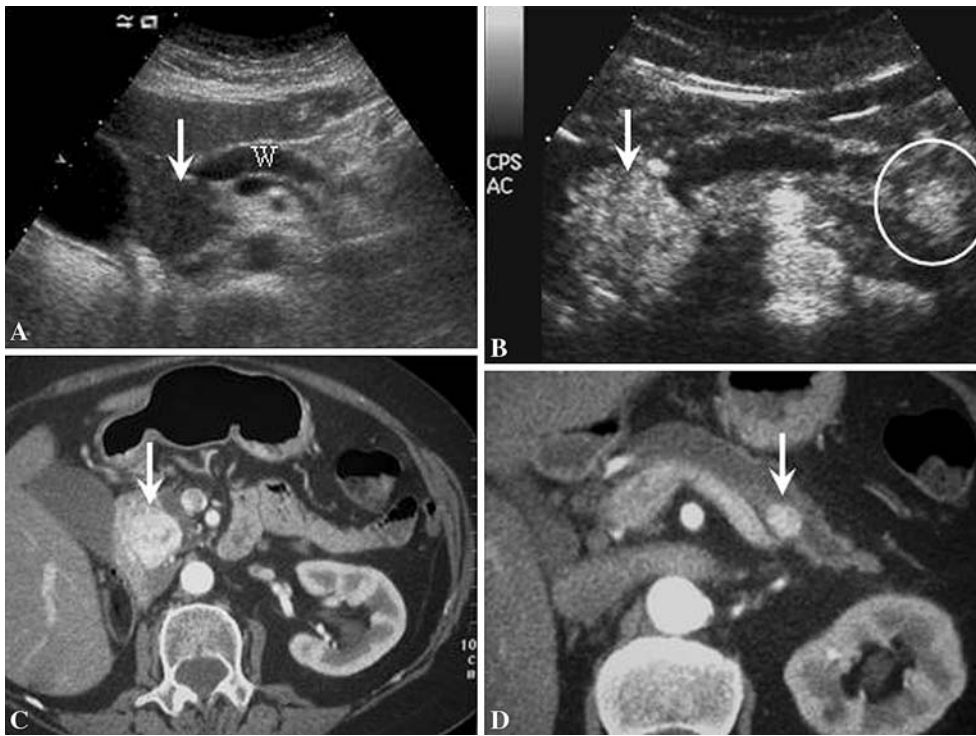


Fig. 9. Pancreatic metastasis. **A** US: pancreatic head hypoechoic solid mass (*arrow*) with upstream pancreatic duct dilatation (W) in a patient with previous right nephrectomy for cancer. **B** CEUS: during the arterial phase the mass appears hypervascular (*arrow*). A second small hypervascular nodule (*circled*) is visible at the pancreatic body. **C, D** MDCT: the hypervascular metastases to the pancreatic head (*arrow* in C) and body (*arrow* in D) are confirmed.

with cystic areas, separated by septa, with a finely corpuscular content due to the presence of mucin. Using tissue harmonic it is possible to better evaluate the walls,

septata, and nodules and the papillary vegetations in the wall, which appear to be better evaluable at US than at single-slice spiral CT [37]. The content of the MCA,

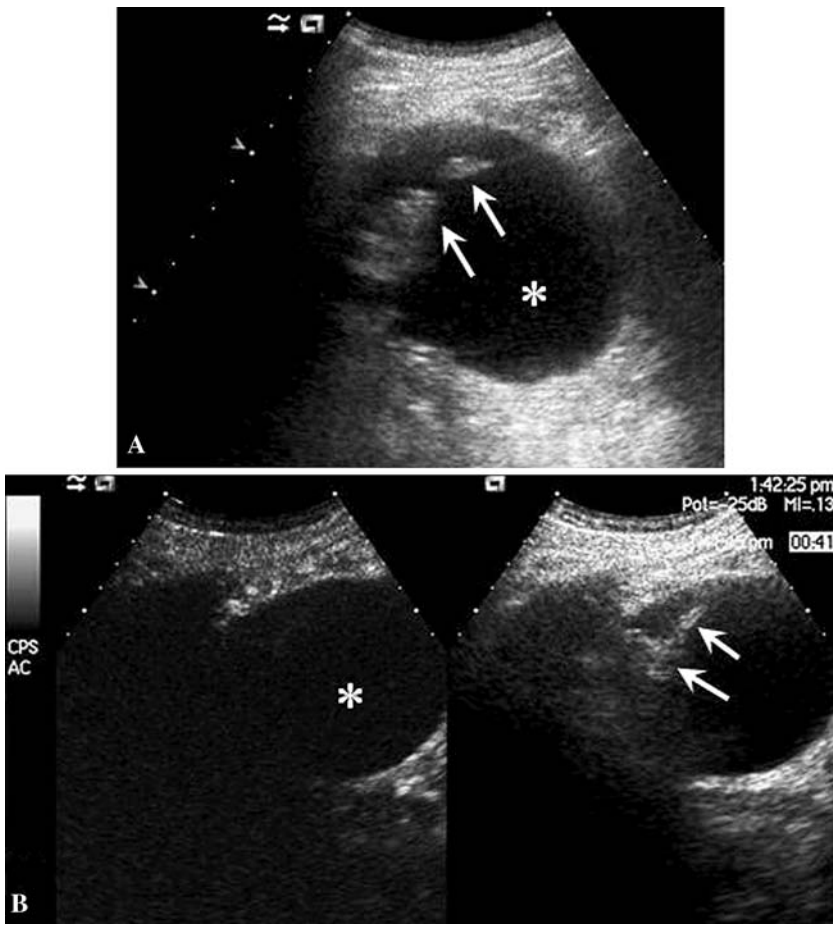


Fig. 10. Pseudocyst. **A** US: cystic pancreatic tail lesion (*asterisk*) with intralesional echoic debris (*arrows*). **B** CEUS: no parietal nodule or septum enhancement inside the lesion, which remains completely and homogeneously anechoic (*asterisk*), is detected. Also, the echoic debris, visible in B mode (*arrow*) at the right part of the screen during the examination performed with the “split-screen” software to correctly study the lesion, does not show any enhancement. The lack of enhancement is consistent with a pseudocyst and rules out the diagnosis of cystic pancreatic tumor.

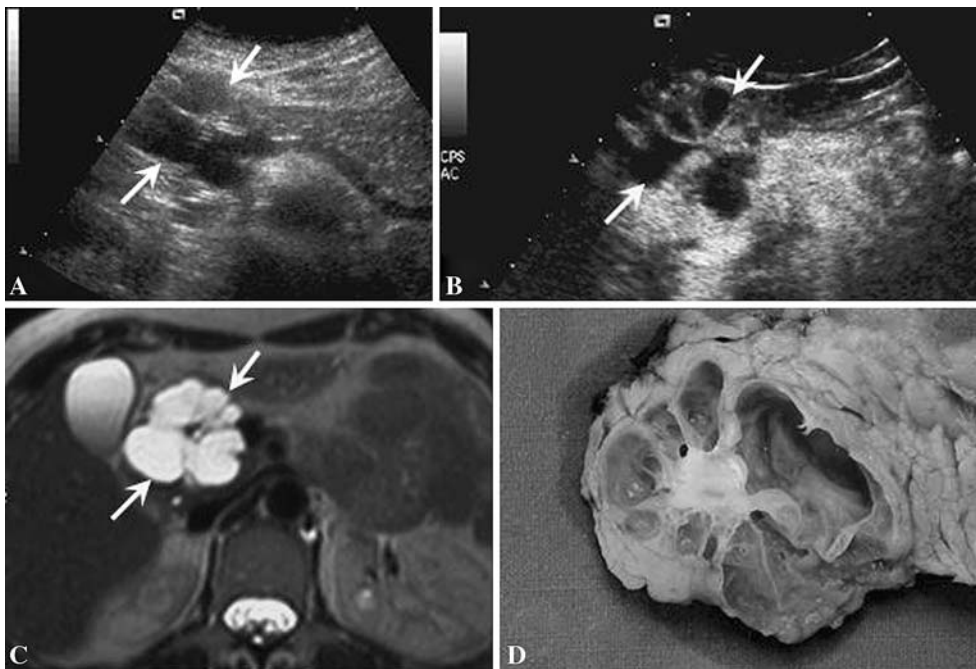


Fig. 11. Serous cystadenoma. **A** US: cystic lesion (*arrows*) with small hyperechoic septa at the pancreatic head. **B** CEUS: septum enhancement with better visualization of the features of this lesion (*arrows*), which is characterized by the presence of numerous well-oriented and centrally directed internal enhancing septa reaching the central portion. **C**, **D** The morphology of the lesion is confirmed at MRI (**C**; *arrows*) and correlates with the resected specimen (**D**) after surgery for obstructive symptoms.

however, if very viscous, may obfuscate identification of parietal nodules, which is fundamental for a radiological diagnosis. CEUS may significantly improve the ultraso-

nographic identification of MCA parietal nodules and septa. In particular, CEUS with second-generation contrast medium, thanks to the dynamic observation of the

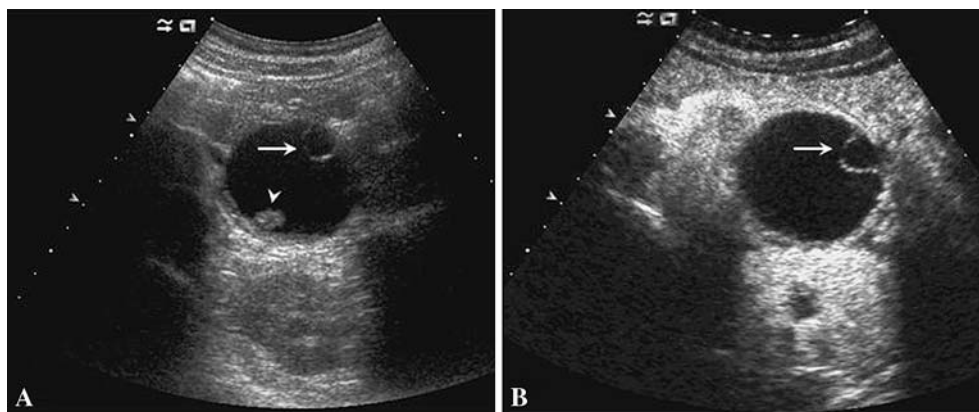


Fig. 12. Mucinous cystoadenoma. **A** US: cystic pancreatic tail mass with a small intralesional septum (arrow) and nodule (arrowhead). **B** CEUS: definite enhancement of the septum (arrow) and no enhancement of the nodule, which represents an intratumoral hemorrhagic clot (surgically proven).

contrast-enhanced phases, allows a demonstration of the enhancement of parietal nodules and intracystic septa, which become hyperechoic (Fig. 12) and stand out against the lesional background, anechoic during the dynamic imaging. CEUS examination, moreover, improves ultrasonographic differential diagnosis between MCA and pseudocyst, thanks to the identification and study of the vascularization of inclusions in cystic masses of the pancreas [10]. IPMTs are considered rare lesions but recently have been reported with increasing frequency [22, 32, 36, 50, 51]. IPMT is macroscopically characterized by intraductal origin and growth [52], with the production of dense mucin that fills the main pancreatic duct (the ductectatic mucin-hypersecreting variant) or with endoluminal papillary proliferation (the papillary-villous variant). US usually demonstrates dilatation of the main pancreatic duct. Ultrasonographic demonstration of the lesion, however, depends on its size. IPMTs of adequate dimensions appear at US as highly inhomogeneous masses, downstream of the main pancreatic duct dilatation, and are difficult to characterize. CEUS examination of the IPMT may allow identification of intraductal papillary tumoral vegetations, especially in the papillary-villous variant, demonstrating its vascularization in the dynamic phase [10] and assisting in the differentiation between benign and malignant lesions [53]. However, a final diagnosis of IPMT by demonstrating the communication between the tumor and the pancreatic duct might be difficult with US [54].

New trends and developments

CEUS is a relatively new imaging modality, which is still evolving. One of the most interesting applications is the possibility of performing tumor characterization and local and liver staging with one single bolus injection of contrast medium. The pancreatic lesion can be studied in the arterial, pancreatic, and venous phases after injection, thus providing characterization according to its perfusion patterns, and local staging thanks to the optimal visualization of the contrast medium-filled vessels.

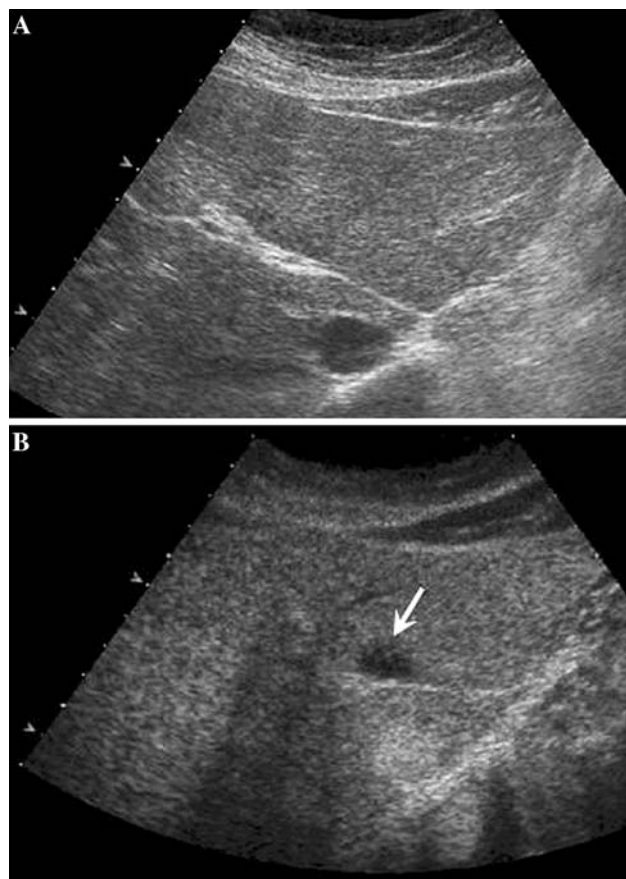


Fig. 13. Liver metastatic pancreatic adenocarcinoma. **A** US: no lesion was visible in the liver during the conventional US examination in a patient with pancreatic body ductal adenocarcinoma. **B** CEUS: a hypoechoic solid metastatic lesion (arrow) was detected in the left lobe of the liver during the sinusoidal phase (120 s after injection) of CEUS.

After this phase, examination of the liver can be performed. The sinusoidal phase of enhancement, 120 s after bolus injection, is the best one for the detection of metastatic liver lesions [55]. Therefore, as abdominal staging is, as a rule, the most important staging workup for pancreatic tumors before surgery [56], CEUS can provide

the information needed to decide whether a patient is a candidate for surgery (Fig. 13).

While characterization and staging in a single examination are now widely used and recognized as feasible, other new trends must be further developed before they can be used. One very promising possibility is the use of CEUS enhancement as a prognostic factor, both in the diagnostic workup and in the follow-up of patients, thanks to its correlation with pathologic features. Another very interesting possibility, still in the first phases of study, is using MBs as a vehicle for targeted therapies [57–59].

References

- D'Onofrio M, Rozzanigo U, Caffarri S, et al. (2004) Contrast-enhanced US of hepatocellular carcinoma. *Radiol Med* 107:293–303
- Quaia E, Stacul F, Gaiani S, et al. (2004) Comparison of diagnostic performance of unenhanced vs SonoVue-enhanced ultrasonography in focal liver lesions characterization. The experience of three Italian centers. *Radiol Med* 108:71–81
- Quaia E, Degobbi F, Tona G, et al. (2004) Differential patterns of contrast enhancement in different focal liver lesions after injection of the microbubble US contrast agent SonoVue. *Radiol Med* 107:155–165
- D'Onofrio M, Mansueto G, Falconi M, Procacci C (2004) Neuroendocrine pancreatic tumor: value of contrast enhanced ultrasonography. *Abdom Imaging* 29:246–258
- Cosgrove D (2004) Advances in contrast agent imaging using Caudence contrast pulse sequencing technology (CPS) and SonoVue. *Eur Rad* 14(Suppl 8)
- Dawson P, Cosgrove DO, Grainger RG (1999) *Textbook of contrast media* Oxford, UK: Isis Medical Media
- D'Onofrio M, Mansueto G, Vasori S, et al. (2003) Contrast enhanced ultrasonographic detection of small pancreatic insulinoma. *J Ultrasound Med* 22:413–417
- Takeda K, Goto H, Hirooka Y, et al. (2003) Contrast enhanced transabdominal ultrasonography in the diagnosis of pancreatic mass lesions. *Acta Radiol* 44:103–106
- Lorén I, Lassin A, Fork T, et al. (1999) New sonographic imaging observations in focal pancreatitis. *Eur Radiol* 9:862–867
- D'Onofrio M, Zamboni G, Malagó R, Martone E, Falconi M, Capelli P, Mansueto G (2005) Pancreatic pathology. In: Quaia E (ed) *Contrast media in ultrasonography*. Springer-Verlag: Berlin, pp 335–347
- D'Onofrio M, Rozzanigo U, Masinielli BM, et al. (2005) Hypoechoic focal liver lesions: characterization with contrast enhanced ultrasonography. *J Clin Ultrasound* 33:164–172
- D'Onofrio M, Martone E, Faccioli N, et al. (2006) Focal liver lesions: sinusoidal phase of CEUS. *Abdom Imaging*, Jun 26; [Epub ahead of print]
- Kim T, Murakami T, Takamura M, et al. (2001) Pancreatic mass due to chronic pancreatitis: correlation of CT and MR imaging features with pathologic findings. *AJR* 177:367–371
- Koito K, Namieno T, Nagakawa T, Morita K (1997) Inflammatory pancreatic masses: differentiation from ductal carcinomas with contrast-enhanced sonography using carbon dioxide microbubbles. *AJR* 169:1263–1267
- Van Gulik TM, Reeders JW, Bosma A, et al. (1997) Incidence and clinical findings of benign, inflammatory disease in patients resected for pancreatic head cancer. *Gastrointest Endosc* 46:417–423
- Remer EM, Baker ME (2002) Imaging of chronic pancreatitis. *Radiol Clin N Am* 40:1229–1242
- Furukawa N, Muranaka T, Yasumori K, et al. (1998) Autoimmune pancreatitis: radiologic findings in three histologically proven cases. *J Comput Assist Tomogr* 22:880–883
- Numata K, Ozawa Y, Kobayashi N, et al. (2004) Contrast enhanced sonography of autoimmune pancreatitis. Comparison with pathologic findings. *J Ultrasound Med* 23:199–206
- Koga Y, Yamaguchi K, Sugitani A, et al. (2002) Autoimmune pancreatitis starting as a localized form. *J Gastroenterol* 37:133–137
- Klößel G, Schlüter E (1999) Pathology of the pancreas. In: Baert AL, Delorme G, Van Hoe L (eds) *Radiology of the pancreas*. 2nd ed. Springer-Verlag: Berlin, pp 69–100
- Oshikawa O, Tanaka S, Ioka T, et al. (2002) Dynamic sonography of pancreatic tumors: comparison with dynamic CT. *AJR* 178:1133–1137
- Ozawa Y, Numata K, Tanaka K, et al. (2002) Contrast-enhanced sonography of small pancreatic mass lesions. *J Ultrasound Med* 21:983–991
- D'Onofrio M, Malago R, Zamboni G, et al. (2005) Contrast-enhanced ultrasonography better identifies pancreatic tumor vascularization than helical CT. *Pancreatol* 5:398–402
- Numata K, Ozawa Y, Kobayashi N, et al. (2005) Contrast-enhanced sonography of pancreatic carcinoma: correlations with pathological findings. *J Gastroenterol* 40:631–640
- Procacci C, Carbognin G, Accordini S, et al. (2001) Nonfunctioning endocrine tumors of the pancreas: possibilities of spiral CT characterization. *Eur Radiol* 11:1175–1183
- Rossi P, Allison DJ, Bezzi M, et al. (1989) Endocrine tumors of the pancreas. *Radiol Clin N Am* 27:129–161
- D'Onofrio M, Malago R, Vecchiato F, et al. (2005) Contrast-enhanced ultrasonography of small solid pseudopapillary tumors of the pancreas: enhancement pattern and pathologic correlation of 2 cases. *J Ultrasound Med* 24:849–854
- Flath B, Rickes S, Schweigert M, et al. (2003) Differentiation of pancreatic metastasis of a renal cell carcinoma from primary pancreatic carcinoma by echo-enhanced power Doppler sonography. *Pancreatol* 3:349–351
- Megibow AJ (2003) Secondary pancreatic tumors: imaging. In: Procacci C, Megibow AJ (eds) *Imaging of the pancreas. Cystic and rare tumors*. Springer-Verlag: Berlin, pp 277–288
- Procacci C, Biasiutti C, Carbognin G, et al. (2001) Pancreatic neoplasms and tumor-like conditions. *Eur Radiol* 11(Suppl 2):S167–S192
- Compagno J, Oertel JE (1978) Mycrocystic adenomas of the pancreas (glycogen-rich cystadenomas). A clinicopathologic study of 34 cases. *Am J Clin Pathol* 69:289–298
- Procacci C, Biasiutti C, Carbognin G, et al. (1999) Characterization of cystic tumors of the pancreas: CT accuracy. *J Comput Assist Tomogr* 23:906–912
- Procacci C, Carbognin G, Biasiutti C, et al. (2001) Serous cystadenoma of the pancreas: imaging findings. *Radiol Med* 102:23–31
- Carbognin G, Tapparelli M, Petrella E, et al. (2003) Serous cystic tumors. In: Procacci C, Megibow AJ (eds) *Imaging of the pancreas. Cystic and rare tumors*. Springer-Verlag: Berlin, pp 31–37
- Procacci C, Graziani R, Bicego E, et al. (1997) Serous cystadenoma of the pancreas: report of 30 cases with emphasis on the imaging findings. *J Comput Assist Tomogr* 21:373–382
- Procacci C, Graziani R, Bicego E, et al. (1996) Intraductal mucin-producing tumors of the pancreas: imaging findings. *Radiology* 198:249–257
- Hammond N, Miller FH, Sica GT, Gore RM (2002) Imaging of cystic disease of the pancreas. *Radiol Clin N Am* 40:1243–1262
- Compagno J, Oertel JE (1978) Mucinous cystic neoplasm of the pancreas with overt and latent malignancy (cystadenocarcinoma and cystadenoma). A clinicopathologic study of 41 cases. *Am J Clin Pathol* 69:573–580
- Cohen-Scali F, Vilgrain V, Brancatelli G, et al. (2003) Discrimination of unilocular macrocystic serous cystadenoma from pancreatic pseudocyst and mucinous cystadenoma with CT: initial observations. *Radiology* 228:727–733
- Buetow PC, Rao P, Thompson LDR (1998) Mucinous cystic neoplasm of the pancreas: radiologic-pathologic correlation. *Radiographics* 18:433–449
- Fugazzola C, Procacci C, Bergamo Andreis IA, et al. (1991) Cystic tumors of the pancreas: evaluation by ultrasonography and computer tomography. *Gastrointest Radiol* 16:53–61
- Sperti G, Cappellazzo F, Pasquali C, et al. (1993) Cystic neoplasm of the pancreas: problems in differential diagnosis. *Am Surg* 59:740–745

43. Demos TC, Posniak HV, Harmath C, et al. (2002) Cystic lesions of the pancreas. *AJR* 179:1375–1388
44. Scott J, Martin I, Redhead D, et al. (2000) Mucinous cystic neoplasm of the pancreas: imaging features and diagnostic difficulties. *Clin Radiol* 55:187–192
45. Sachs JR, Deren JJ, Sohn M, Nusbaum M (1989) Mucinous cystadenoma: pitfalls of differential diagnosis. *Am J Gastroenterol* 84:811–816
46. Kuba H, Yamaguchi K, Shimizu S, et al. (1998) Chronic asymptomatic pseudocyst with sludge aggregates masquerading as mucinous cystic neoplasm of the pancreas. *J Gastroenterol* 33:766–769
47. De Lima JE Jr, Javitt MC, Mathur SC (1999) Residents' teaching files: mucinous cystic neoplasm of the pancreas. *Radiographics* 19:807–811
48. Procacci C, Carbognin G, Accordini S, et al. (2001) CT features of malignant mucinous cystic tumors of the pancreas. *Eur Radiol* 11:1626–1630
49. D'Onofrio M, Caffarri S, Zamboni G, et al. (2004) Contrast-enhanced ultrasonography in the characterization of pancreatic mucinous cystadenoma. *J Ultrasound Med* 23:1125–1129
50. Procacci C, Megibow AJ, Carbognin G, et al. (1999) Intraductal papillary mucinous tumor of the pancreas: a pictorial essay. *Radiographics* 19:1447–1463
51. Procacci C, Carbognin G, Biasiutti C, et al. (2001) Intraductal papillary mucinous tumors of the pancreas: spectrum of CT and MR findings with pathologic correlation. *Eur Radiol* 11:1939–1951
52. Zamboni G, Capelli P, Bogina G, et al. (2003) Pathology of intraductal cystic tumors. In: Procacci C, Megibow AJ (eds) *Imaging of the pancreas. Cystic and rare tumors*. Springer-Verlag: Berlin, pp 85–94
53. Itoh T, Hirooka Y, Itoh A, et al. (2005) Usefulness of contrast-enhanced transabdominal ultrasonography in the diagnosis of intraductal papillary mucinous tumors of the pancreas. *Am J Gastroenterol* 100:144–152
54. Procacci C, Schenal G, Della Chiara E, et al. (2003) Intraductal papillary mucinous tumors: imaging. In: Procacci C, Megibow AJ (eds) *Imaging of the pancreas. Cystic and rare tumors*. Springer-Verlag: Berlin, pp 97–137
55. EFSUMB Study Group (2004) Guidelines for the use of contrast agents in ultrasound. *Ultrasound Med* 25:249–256
56. Nordback I, Saaristo R, Piironen A, Sand C (2004) Chest computed tomography in the staging of pancreatic and periampullary carcinoma. *Scand J Gastroenterol* 39:81–86
57. Nakaya H (2005) Microbubble-enhanced ultrasound exposure promotes uptake of methotrexate into synovial cells and enhanced antiinflammatory effects in the knees of rabbits with antigen-induced arthritis. *Arth Rheum* 52:2559–2566
58. Liu Y, Yang H, Sakanishi A (2005) Ultrasound: mechanical gene transfer into plant cells by sonoporation. *Biotechnol Adv* 24:1–16
59. van Wamel A, Bouakaz A, Bernard B, et al. (2005) Controlled drug delivery with ultrasound and gas microbubbles. *J Control Release* 101:389–391